Spray and Mixture Formation Processes by High-Pressure Swirl Injector for DISI Engine - Analyses Based on Laser Absorption Scattering (LAS) Measurements

T. LI[1], M. YAMAKAWA[2], K. NISHIDA[3*], D. TAKAKI[3], Y. ZHANG[3] and H. HIROYASU[1]

[1]Graduate School of Industrial Technology, Kinki University
Takaya Umenobe 1, Higashi-Hiroshima 739-2116, Japan

[2]Mazda Motor Corporation, 3-1 Shinchi, Fuchu-cho, Aki-gun, Hiroshima 730-8670, Japan

[3]Department of Mechanical System Engineering, University of Hiroshima
1-4-1 Kagamiyama, Higashi-Hiroshima 739-8527, Japan

Mixture formation process plays a vital role on the combustion and emission formation processes in a Direct Injection Spark Ignition (DISI) engine. Quantitative measurement of the mixture concentration distribution in the spray is essential in understanding the mixture formation process. In this study, the Laser Absorption Scattering (LAS) technique was employed to quantitatively and simultaneously measure the concentration distributions of both the liquid and vapor phases in the fuel spray injected by the high-pressure swirl injector for DISI engine. P-xylene, which is suitable for the LAS technique and has similar properties to gasoline, was injected by the injector into a high pressure and high temperature constant volume vessel. Based on the LAS measurements of the temporal variations of the concentration distributions in the fuel spray, the spray and mixture properties, such as mass of vapor/liquid phases and entrained ambient air in the entire spray, overall equivalence ratio of the mixture, ratio of evaporated fuel, were analyzed. Injection condition parameters, such as injection pressure and injection splitting, were examined. It was found that the higher injection pressure enhances the atomization of the fuel spray, increases the ambient air entrainment, as well as the evaporation rate, and eventually improves the mixing of the fuel and the entrained air. Increasing the dwell in the split injection increases the air entrained into the spray and decreases the overall equivalence ratio of the mixture.

1 Introduction

Spray and mixture preparation processes are very important for DISI engine, especially, instead of the wall-guided concept [1,2], the air- and spray-guided concepts [3-7] were recently reported to have more potential for the DISI engine in the future. However, quantitative measurement of transient spray concentration distribution is very difficult. Zhao et al. [8] conducted a study on the vapor concentration of gasoline sprays by the laser Rayleigh scattering technique, which is based on the elastic light scattering of gas molecules. Obviously, the existence of liquid phase in the mixture negates much of the measurement accuracy. Rabenstein [9] et al. quantitatively analyzed the vapor phase structures by the linear Raman scattering technique. However, besides the limitations of one-dimensional linear measurement and signal weakness, the Raman scattering technique also suffers from signal scattering of fuel droplets, and it is limited to only vapor phase measurement. Laser-induced fluorescence (LIF) is a technique widely used in the concentration distribution measurement of a spray [10, 11]. However, the LIF technique cannot make simultaneous measurements of both the liquid and vapor phases in a spray. It is also is very difficult to get quantitative information on a spray using LIF. Melton developed a laser-induced exciplex fluorescence (LIEF) technique [12], and measured simultaneously the liquid and vapor phases in a diesel spray [13]. Many researchers are now employing the LIEF technique to study gasoline sprays [4, 14, 15]. However, LIEF is a temperature dependent method, and must also overcome fluorescence quenching by oxygen in the mixture. Additionally, this method suffers from the overlap of the fluorescence signals of the liquid and vapor phases. Laser absorption and scattering technique (LAS) was initially proposed by Chraplyvy [16] to measure the vapor fraction in a fuel spray in the presence of liquid droplets using infrared and visible lasers. Later, the LAS technique was developed to gather simultaneous and quantitative measurements of liquid and vapor phase concentration distributions in a

* Corresponding author

diesel spray [17, 18] as well as a gasoline spray [19]. Although the LAS technique has some drawbacks due to the line-of-sight arrangement, it shows great promise as a measurement method of the evaporating process of a fuel spray.

In this paper, firstly, the principle of the LAS technique is stated concisely. Then the LAS system setup is described. Finally, based on the LAS experiments, the temporal variations of the concentration distribution, and the effects of injection conditions, such as injection pressure and injection splitting on the concentration distribution of both liquid and vapor phase in the spray are investigated.

2 Principle of laser absorption scattering (LAS) technique

A two-wavelength (l_A: absorption wavelength, l_T: transparent wavelength) incident light of intensity of I_0 is transmitted through a mixture of both vapor and liquid phase, and is attenuated into a transmitted light of intensity I_t. The extinction of absorption wavelength light is attributed to liquid phase scattering and absorption $\log(I_0/I_t)_{Lsca+Labs}$ as well as vapor phase absorption $\log(I_0/I_t)_{Vabs}$, and its extinction rate $\log(I_0/I_t)_{lA}$ is defined by Eq. (1). The extinction of transparent light is attributed to only the liquid phase scattering $\log(I_0/I_t)_{Lsca}$ and its extinction rate $\log(I_0/I_t)_{lT}$ is defined by Eq. (2).

$$\log\left(\frac{I_0}{I_t}\right)_{l_A} = \log\left(\frac{I_0}{I_t}\right)_{Lsca+Labs} + \log\left(\frac{I_0}{I_t}\right)_{Vabs} \tag{1}$$

$$\log\left(\frac{I_0}{I_t}\right)_{l_T} = \log\left(\frac{I_0}{I_t}\right)_{Lsca} \tag{2}$$

If the extinction of both of the two wavelengths light of the liquid phase is the same (This has been testified to in the previous work [19]), the extinction rates of the vapor phase absorption and the liquid phase scattering can be expressed as Eqs. (3) and (4), respectively.

$$\log\left(\frac{I_0}{I_t}\right)_{Vabs} = \log\left(\frac{I_0}{I_t}\right)_{l_A} - \log\left(\frac{I_0}{I_t}\right)_{l_T} \tag{3}$$

$$\log\left(\frac{I_0}{I_t}\right)_{Lsca} = \log\left(\frac{I_0}{I_t}\right)_{l_T} \tag{4}$$

Based on Lambert-Beer's law and Eq. (3), the concentration of vapor phase C_v [kg/m^3] can be expressed as Eq. (5).

$$\int_0^l C_v\,dx = \frac{1}{\varepsilon}\cdot\frac{MW}{10^2}\log\left(\frac{I_0}{I_t}\right)_{Vabs} \tag{5}$$

The optical path length l and the extinction rate $\log(I_0/I_t)_{Vabs}$ can be determined by experiment, the mole weight MW is dependent on the fuel, and if the molar absorption coefficient ε of the fuel is known, the vapor concentration distribution can be obtained.

Based on Bouguer-Lambert-Beer's law and Eq. (4), the concentration of liquid phase C_l [kg/m^3] can be derived as Eq. (6).

$$\int_0^l C_l\,dx = \frac{2}{3}\cdot\rho_f\cdot\frac{D_{32}}{R\cdot Q_{ext}}\cdot 2.303\cdot\log\left(\frac{I_0}{I_t}\right)_{Lsca} \tag{6}$$

The fuel density ρ_f is dependent on the physical properties. If the size of the droplets is sufficiently large compared to the wavelength, the extinction efficiency Q_{ext} approaches a value of 2 [20]. In addition, when the distance between the droplets cloud and a camera is sufficiently larger than the field depth of the droplets cloud, the optical constant R tends to be a value of 0.6 [21]. In this experimental system, the above two conditions are met [22]. The Sauter mean diameter D_{32} is given by Eq. (7) and can be determined experimentally [19].

$$D_{32} = \frac{0.63 \cdot R \cdot Q_{ext} \cdot M_{fl}}{r_f \cdot \sum_S \left[\log\left(\frac{I_0}{I_t} \right)_{Lsca} \Delta S \right]} \quad (7)$$

In order to get spatial distributions of the liquid and vapor phase concentrations from the line-of-sight LAS images, the onion-peeling model was adopted. The detailed deconvolution process can be found in the previous work [19].

3 Experimental setup

Figure 1 shows the schematic of the LAS experimental setup. A pulsed Nd:YAG laser was employed to provide two-wavelength beams, one at ultraviolet band 266 nm and the other at visible band 532 nm. The two beams were separated by a dichroic mirror, and were magnified to a diameter of 100 mm by beam expanders. Then the two beams were combined into a coaxial beam by a dichroic mirror, and beamed through the constant volume vessel, transmitted through the spray and separated again on the other side. In order to minimize the schlieren-like effect due to the ambient gas density gradient on the LAS image, a diffuser is set between the first dichroic mirror and the window of the vessel. Finally, the two beams were focused and captured by two CCD cameras. The images were transferred to a computer for LAS image analysis. In the injection system, a swirl type injector for DISI engine use was employed, which has a cone angle of 50 degrees at one atmospheric pressure. P-Xylene, which has been proven to

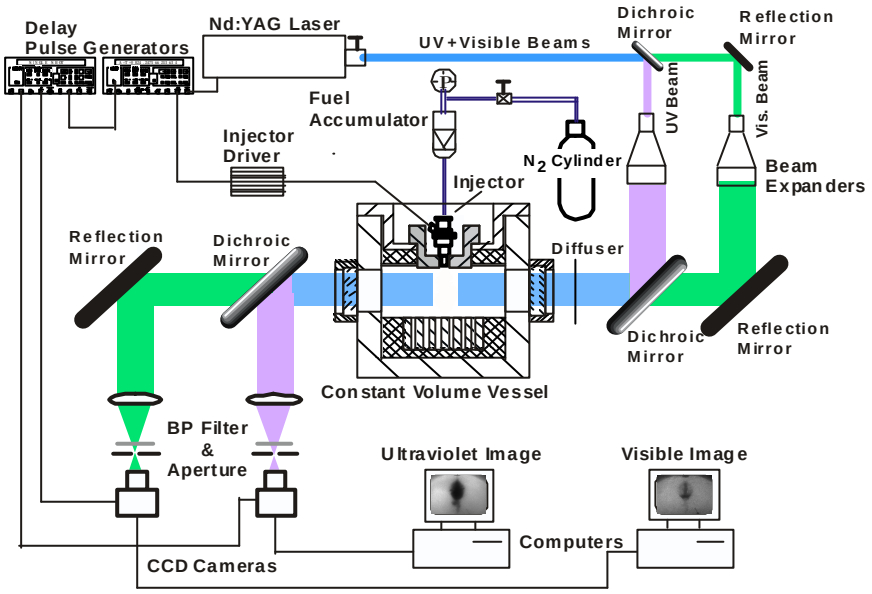

Fig. 1 Experimental Setup of LAS System, Fuel Injection System and Constant Volume Vessel

Table 2 Experimental Conditions

Ambient Gas	Nitrogen
Ambient Pressure	1.0 MPa
Ambient Temperature	500 K
Injector Type	Swirl Injector
Test Fuel	p-Xylene
Single Injection	
Quantity Injected (mg)	6.0
Pressure (MPa)	3, 5, 7
Duration* (ms)	1.08, 0.9, 0.76
Split Injection	
Total Quantity Injected (mg)	14.0
Pressure (MPa)	5
Dwell* (ms)	0, 0.5, 1.0
Total Injection Duration* (ms)	2.0

* Control Pulse

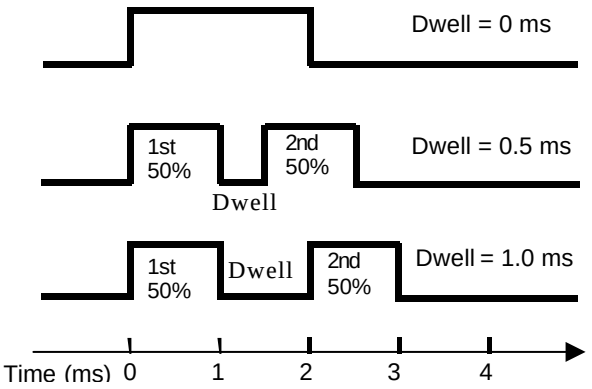

Fig. 2 Time Chart of Control Pulse for Split Injection

be suitable to the application of the LAS technique, was selected as the test fuel [19]. The laser firing, injection and CCD shuttering timings were controlled by delay pulse generators.

Experimental conditions are shown in Table 1. Nitrogen was used as the ambient gas. The ambient pressure and temperature were 1.0 MPa and 500 K. For the single injection, injection pressures of 3, 5, and 7 MPa and corresponding injection durations of 1.08, 0.9 and 0.76 ms were set to investigate the injection pressure's effect on the concentration distribution in the spray. For the split injection, the injection pressure was fixed at 5.0 MPa, and two pulses with each of 1ms duration were proposed. The dwell width of 0, 0.5 and 1.0 ms between the two pulses were set to investigate its effect on the mixture formation. A time chart of split injection is shown in Fig. 2.

4 Results and discussion

4.1 Temporal variations of liquid and vapor phase equivalence ratio distributions

Figure 3 shows the temporal variations of liquid and vapor phase equivalence ratio distributions in the spray as a baseline compared with other injection conditions. The imaging timings are 1, 2, 3, and 4 ms after the start of injection. The left hand side of the image at each time in Fig. 3 shows the liquid phase and the right hand side shows the vapor phase. At 1 ms after the start of injection, an initial spray is clearly found centered below the main spray in the liquid phase, and almost no evaporation occurs due to the short time. At 2 ms, there is shown a high equivalence ratio of vapor phase in the initial spray. This may be attributed to the fact that the poorly atomized initial spray broke up and formed a droplets cluster under high ambient pressure conditions [23], and vaporized quickly as it interacted with the ambient gas at high temperature. In the main spray region, the highest equivalence ratio does not distribute in the axial region, but in a certain distance from the spray axis, where the counter-rotating vortexes are supposed to exist [24] and take small droplets there. At 3.0 and 4.0 ms, the liquid phase fuel decreases gradually and the vapor phase fuel distributes more extensively. Interestingly, the vapor phase spray penetrates along the axial direction but there is almost no extension along the radial direction. This may be attributed to the fact that the vapor phase is affected more easily by the ambient air motion, and the high ambient pressure suppresses the air motion along radial direction.

Figure 4 shows the temporal variations of mass of liquid, vapor, and air entrained into the spray. As time proceeded, the spray evaporated, the mass of liquid phase fuel decreased, and the mass of vapor phase fuel increased gradually, and the mass of ambient air entrained into the spray also increased. The ratio of evaporated fuel increased, and overall equivalence ratio of the spray decreased with time as

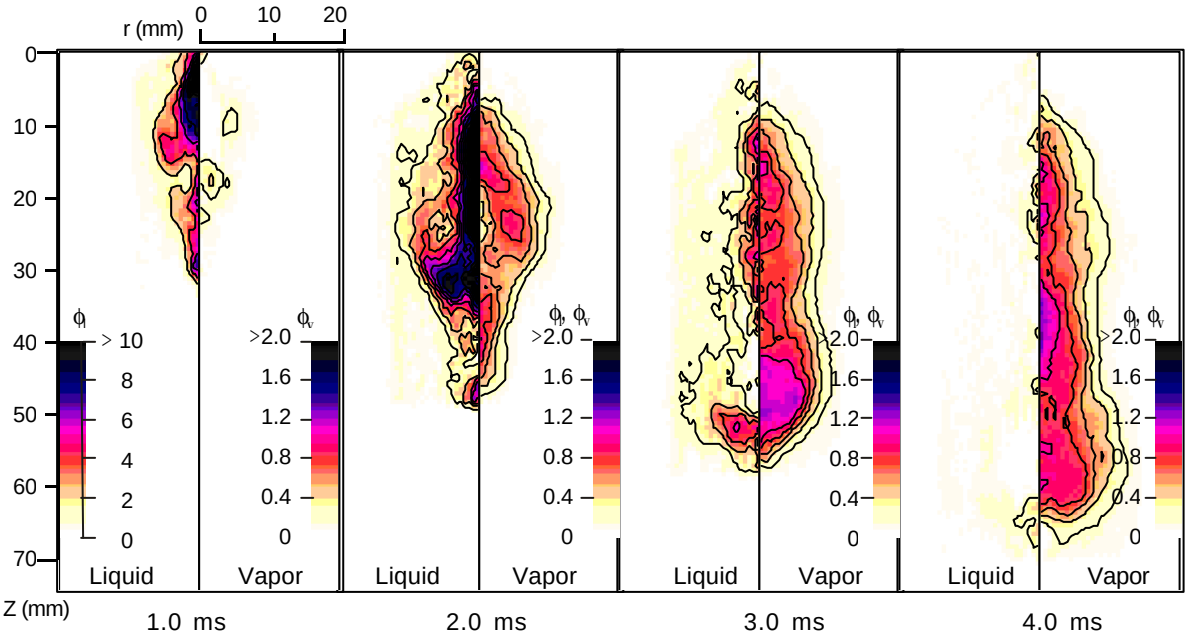

Fig. 3 Temporal Variations of Liquid and Vapor Phase Equivalence Ratio Distributions (P_a=1.0MPa, T_a=500K, P_{inj}=5MPa, M_f=6.0mg, t_{inj}=0.9ms)

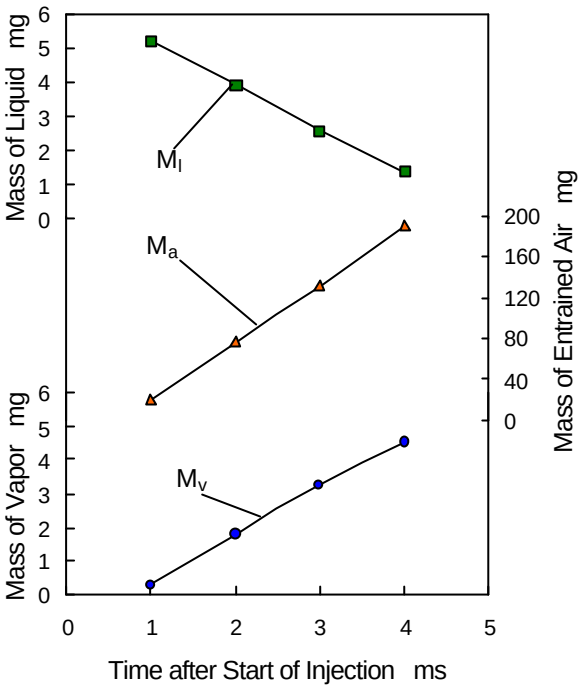

Fig. 4 Temporal Variations of Mass of Liquid, Vapor, and Entrained Air in the Spray (P_a=1.0MPa, T_a=500K, P_{inj}=5MPa, M_f=6.0mg, t_{inj}=0.9ms)

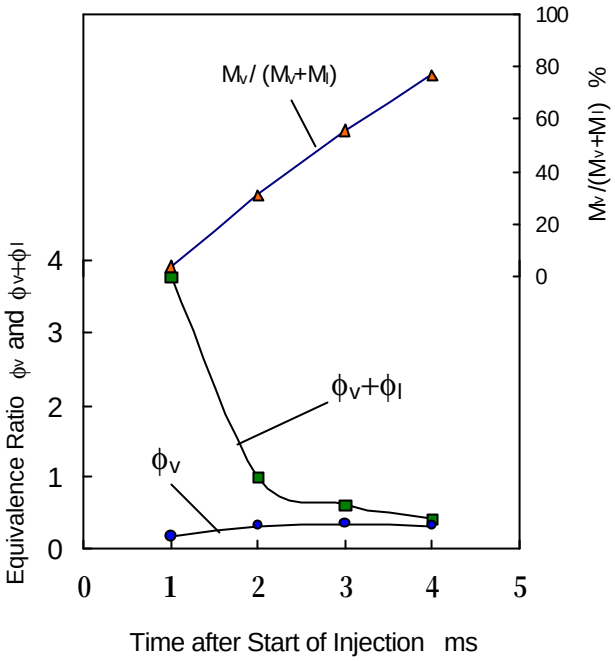

Fig. 5 Temporal Variations of Equivalence Ratio $\phi_v+\phi_l$, ϕ_v, and Mass Ratio of Vapor (P_a=1.0MPa, T_a=500K, P_{inj}=5MPa, M_f=6.0mg, t_{inj}=0.9ms)

shown in Fig. 5. The overall equivalence ratio is defined by the sum of the liquid and vapor phase equivalence ratio of the whole spray, that is, f_l+f_v. It should be noted that the curve of overall equivalence ratio shows a steep decline before 2 ms and then evens out. This may be attributed to the fact that the droplets had a relative higher penetration velocity early in the injection and induced strong ambient air motion, as well as increased the evaporation rate and mass of air entrained into the spray.

4.2 Effect of injection pressure on mixture formation

In order to optimize the mixture formation and combustion processes in a DISI engine, the injection pressure can be changed to correspond to different engine speeds. However, when the injection pressure is increased, the spray will penetrate a farther distance, the problems of engine cylinder wetting and piston surface impingement will be encountered, especially for the air- and spray-guided concepts, in

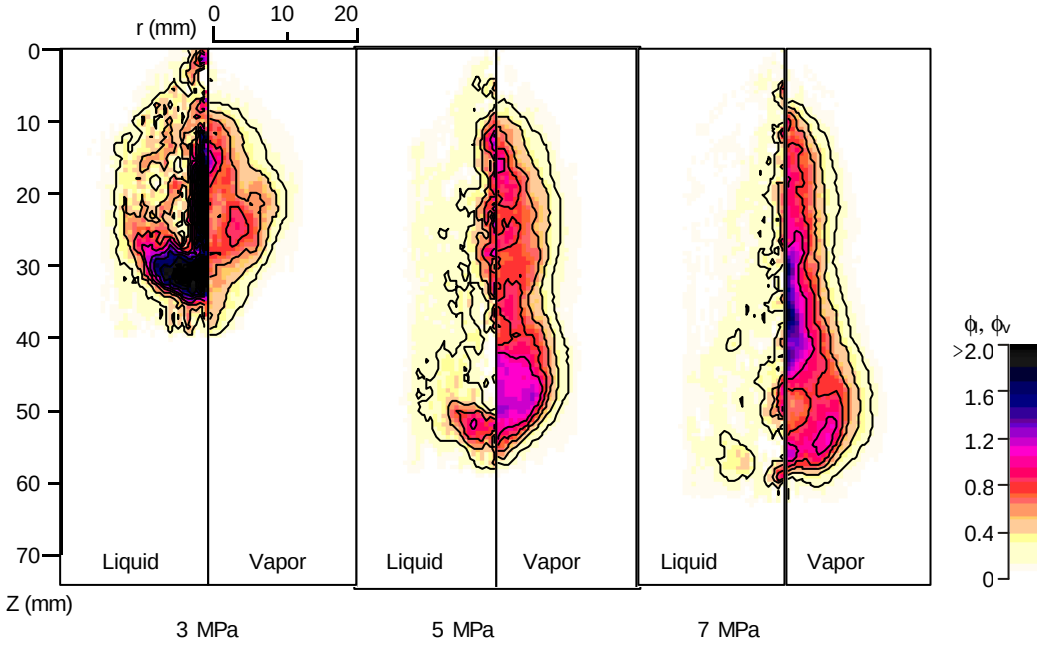

Fig. 6 Effect of Injection Pressure on Equivalence Ratio Distributions (P_a = 1.0 MPa, T_a = 500 K, M_f = 6.0 mg, t_{SOI} = 3.0 ms)

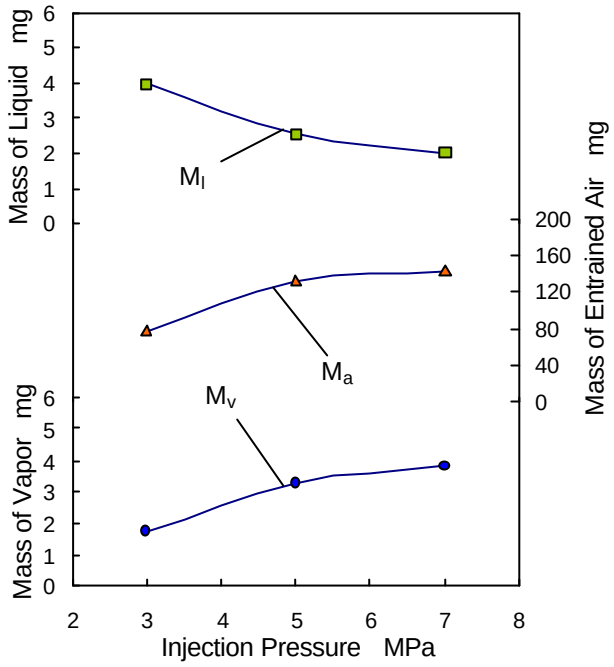

Fig. 7 Effect of Injection Pressure on Mass of Liquid, Vapor and Entrained Air (P_a = 1.0 MPa, T_a = 500 K, M_f = 6.0 mg, t_{SOI} = 3.0 ms)

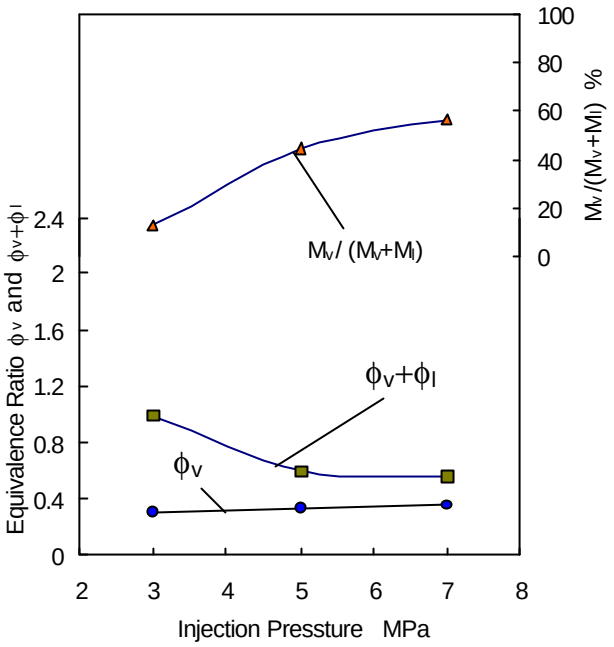

Fig. 8 Effect of Injection Pressure on Equivalence Ratio $\phi_v+\phi_l$, ϕ_v, and Mass Ratio of Vapor (P_a = 1.0 MPa, T_a = 500 K, M_f = 6.0 mg, t_{SOI} = 3.0 ms)

which no cylinder wetting and piston surface impingement are reported to be the attractive advantages. Therefore, the effect of injection pressure on the mixture formation processes was investigated.

Figure 6 shows the effect of injection pressure on the equivalence ratio distributions of both the liquid and vapor phases in the sprays. The imaging timing is 3 ms after the start of injection. Compared to those with an injection pressure of 3 MPa, the sprays with an injection pressure of 5 and 7 MPa penetrate farther, and show a higher equivalence ratio of vapor phase fuel. It can be considered that the higher injection pressure enhances the atomization of the spray, induces stronger ambient air motion, and eventually increases the evaporation rate. However, when the spray in case of injection pressure 5 MPa is compared to that of 7 MPa, the difference is small.

Figure 7 shows the effect of injection pressure on the mass of liquid, vapor, and entrained air. It is not difficult to find that the mass of liquid phase fuel will decrease and the mass of vapor phase fuel will increase with increasing injection pressure. However, it should be noted that when the injection pressure is increased from 5 to 7 MPa, the variation of mass of liquid or vapor phase fuel in the spray is not very apparent compared to that between 3 to 5 MPa. This can be explained by the fact that the higher injection pressure can promote the atomization of spray, but when the injection pressure is increased above 5 MPa, the effect becomes small. Nevertheless, higher pressure can promote ambient air motion, and increase the air entrained into the spray, which subsequently results in the reduction of the overall equivalence ratio of the spray as shown in Fig. 8. This may help to avoid an over rich mixture.

4.3 Effect of split injection on mixture formation

Split injection strategy has been adopted in production engine [1, 25], and has been studied and evaluated by many researchers [26, 27]. However, when the split injection is used for stratified mixture, the issues such as time-resolved local mixture concentration distribution and so on must be carefully addressed.

In this work, the effect of dwell width between the two pulses on the mixture formation was investigated. The injection conditions and time chart is shown in previous section. Figure 9 shows the effect of split injection on the equivalence ratio distributions at 3ms after the start of injection. For the split injection, the liquid fuel sprays are apparently split into two parts, and the whole spray penetrats shorter than that of single injection. Compared to the case of dwell 0.5 ms, that of dwell 1.0 ms shows the highest equivalence ratio in the region between the separated liquid sprays.

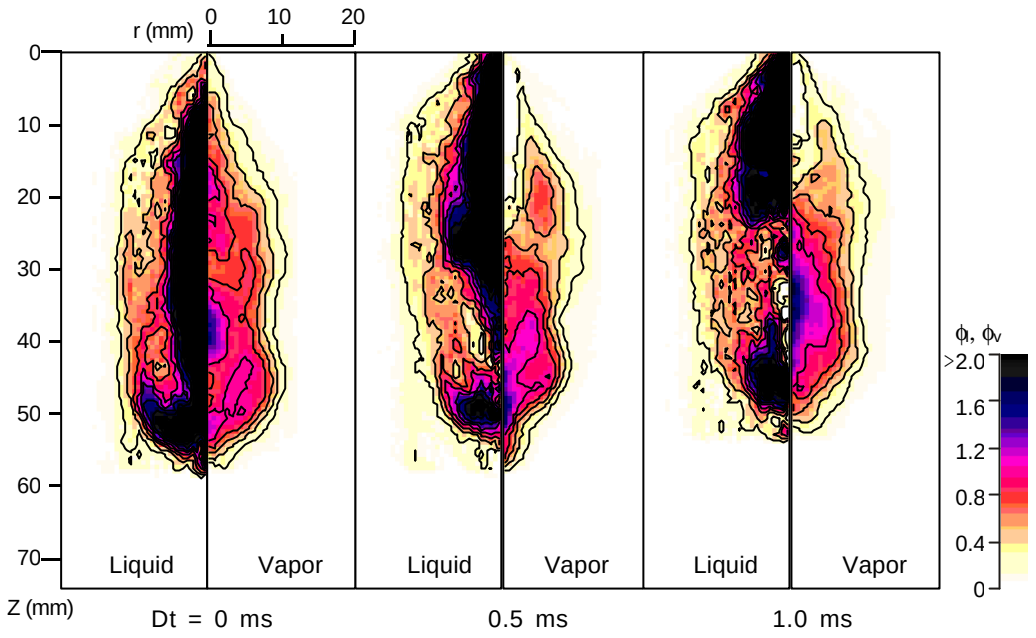

Fig. 9 Effect of Split Injection on Equivalence Ratio Distributions (P_a = 1.0 MPa, T_a = 500 K, M_f = 6.0 mg, t_{SOI} = 3.0 ms)

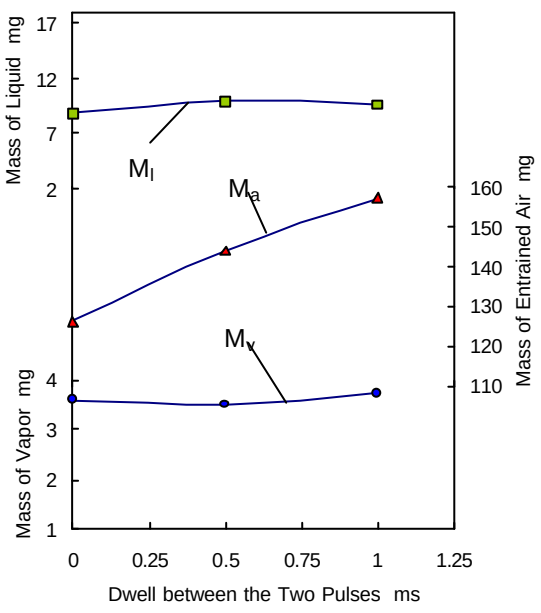

Fig. 10 Effect of Split Injection on Mass of Liquid, Vapor and Entrained Air (P_a = 1.0 MPa, P_{inj} = 5MPa, T_a = 500 K, t_{SOI} = 3.0 ms)

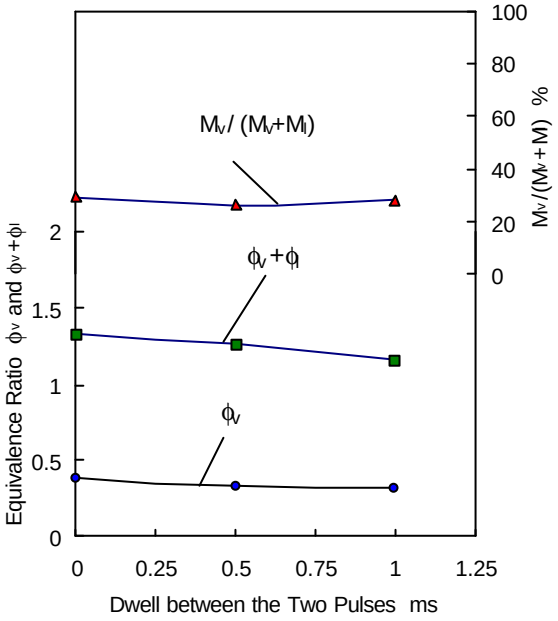

Fig. 11 Effect of Split Injection on Equivalence Ratio $\phi_v+\phi_l$, ϕ_v, and Mass Ratio of Vapor (P_a = 1.0 MPa, P_{inj} = 5MPa, T_a = 500 K, t_{SOI} = 3.0 ms)

Figure 10 shows the effect of split injection on the mass of liquid, vapor and entrained air. When the dwell is increased, the mass of liquid and vapor phase in the spray do not changed very much, but the mass of air entrained into the spray apparently increases. This causes the overall equivalence ratio decrease as shown in Fig. 11. The ratio of evaporated fuel and equivalence ratio of vapor phase in the spray do not change very apparently.

5 Conclusions

In this paper, the laser absorption and scattering (LAS) technique was employed to study the spray and mixture formation processes of the fuel spray by the swirl injector for a DISI engine. Effects of injection

conditions, such as injection pressure and dwell for split injection, on the liquid and vapor phase concentration distributions in the sprays were investigated. Mass of vapor/liquid phase fuel and the air entrained into the spray, and overall equivalence ratio of the spray, were analyzed. The results are concluded as follows:

- During the 1 ms after the end of injection, the overall equivalence ratio $\phi_v+\phi_l$ of the spray decreases quickly from an equivalence ratio 4.0 to a value less than 1.0. The mass of vapor phase fuel and air entrained into the spray increase, and the mass of liquid phase fuel decreases.
- When the spray almost evaporates completely and there is little liquid phase fuel left in the spray, the vapor-air mixture distribution is extended along the spray axis direction, though not much in the radial direction.
- Higher injection pressure increases the evaporation rate of the spray, promotes the air-fuel mixture formation, enhances air entrainment, and avoids the over rich mixture. However, meanwhile the spray penetration is increased.
- When the dwell between the pulses is increased, the split injection can increase air entrained into the spray, and decrease the overall equivalence ratio of the spray.

References

1. Harada, J., Tomita, T., Mizuno, H., Mashiki, Z. and Ito, Y. 1997 *SAE Technical Paper*, No. 970540
2. Iwamoto, Y., Noma, K., Nakayama, T., Yamauchi, T. and Ando, H. 1997 *SAE Technical Paper*, No. 970451
3. Geiger, J., Grigo, M., Lang, O., Wolters, P. and Hupperich, P. 1999 *SAE Technical Paper*, No. 1999-01-0170
4. Ortmann, R., Arndt, S., Rainmann, J., Grzeszik, R. and Wurfel, G. 2001 *SAE Technical Paper*, No. 2001-01-0970
5. Georjon, T., Bourguignon, E., Duverger, T., Delhaye, B. and Voisard, P 2000, *SAE Technical Paper*, No. 2000-01-0534
6. Cathcart, G. and Zavier, C. 2000 *SAE Technical Paper*, No. 2000-01-0256
7. Schanzlin, K., Kock, T. and Boulouchos, K 2002 *SAE Technical Paper*, No. 2002-01-0834
8. Zhao, F., Taketomi, M., Nishida, K. and Hiroyasu, H. 1993 *SAE Technical Paper*, No. 932641
9. Rabenstein, F., Egermann, J. and Leipertz, A 1998 *The 4th International Symposium COMODIA*
10. VanDerWege, B., and Hochgreb, S 2000 *SAE Technical Paper*, No. 2000-01-0535
11. Davy, M., Williams, P., and Anderson, R. 2000 *SAE Technical Paper*, No. 2000-01-1904
12. Melton, L. 1983 *Applied Optics*, Vol. 22, No. 14/15, p. 2224
13. Melton, L. and Verdieck, J. 1984 *20th Symposium (International) on Combustion*, pp.1283-1290,
14. Styron, J., Kelly-Zion, P., Lee, C., Peters, J. and White, R. 2000 *SAE Technical Paper*, No. 2000-01-0243
15. Ipp, W., Wagner, V., Kramer, H., Wensing, M., Leipertz, A., Arndt, S. and Jain, A. 1999 *SAE Technical Paper*, No. 1999-01-0498
16. Chraplyvy, A. 1981 *Applied Optics*, Vol. 20, No. 15, pp.2620-2624
17. Suzuki, S., Nishida, K. and Hiroyasu, H. 1993 *SAE Technical Paper*, No. 930863
18. Zhang, Y., Yoshizaki, Y. and Nishida, K. 2000 *Applied Optics*, Vol. 39, No. 33, pp. 6221-6229
19. Yamakawa, M., Takaki, D., Li, T., Zhang, Y. and Nishida, K. 2002 *SAE Technical Paper*, No. 2002-01-1644
20. Van de Hust, H. *Light Scattering by Small Particles*, 1957 A Jone&Sons, Inc., Publication
21. Twomey, S., Howell, H.B. 1965 *Applied Optics*, Vol. 4, No. 4, pp. 501
22. Yamakawa, M: *2001 Ph. D thesis*, University of Hiroshima
23. Li, T, Nishida, K. and Hiroyasu, H. 2003 *Atomization and Sprays*, to be published
24. Yamakawa, M., Isshiki, T., Yoshizaki, T. and Nishida, K.: 2001 *the 5th COMODIA*, pp. 499-504
25. Kuwahara, K., Ueda, K. and Ando, H 1998 *SAE Technical Paper*, No. 980158
26. Yang, J. and Anderson, R.W. 1998 *SAE Technical Paper*, No. 980495
27. Stiesch, G., Merker, G.P., Tan, Z. and Reitz, R.D. 2001 *SAE Technical Paper*, No. 2001-01-0956